Supplement of Atmos. Chem. Phys., 22, 13753–13782, 2022
https://doi.org/10.5194/acp-22-13753-2022-supplement

Atmospheric Chemistry and Physics
Open Access
EGU

Supplement of

Global tropospheric ozone trends, attributions, and radiative impacts in 1995–2017: an integrated analysis using aircraft (IAGOS) observations, ozonesonde, and multi-decadal chemical model simulations

Haolin Wang et al.

Correspondence to: Xiao Lu (luxiao25@mail.sysu.edu.cn) and Shaojia Fan (eesfsj@mail.sysu.edu.cn)

Table S1. Seasonal biases (ppbv) between observed and modeled lower tropospheric ozone (950-800 hPa) for 11 IAGOS regions from 1995-1999 to 2013-2017.

Region	1995-1999				2013-2017			
	MAM	JJA	SON	DJF	MAM	JJA	SON	DJF
East Asia	-7.6	9.3	1.6	-7.4	-10.5	4.6	-0.4	-10.1
India	13.6	8.1	15.3	16.2	4.9	6.4	2.8	4.8
Southeast Asia	6.9	11.3	14.3	11.2	1.1	3.1	11.4	5.6
Persian Gulf	5.7	12.5	19.7	4.3	0.4	9.5	13.7	-0.1
Malaysia/Indonesia	7.5	9.3	24.5	14.5	0.8	-1.3	0.4	4.6
Gulf of Guinea	10.3	5.6	10.2	18.2	-7.6	-2.4	1.3	-1.2
Northern South America	3.8	0.8	1.8	7.1	-12.5	-6.2	2.3	5.1
Europe	-3.6	8.7	1.8	-4.7	-4.1	3.9	0.9	-6.6
Eastern North America	2.0	13.0	10.1	-1.5	-1.8	5.8	6.7	-2.1
Southeast US	7.6	15.7	10.4	2.8	-3.5	4.5	3.1	0.3
Western North America	-3.2	13.0	3.4	-4.4	-9.9	-4.1	-6.1	-9.5

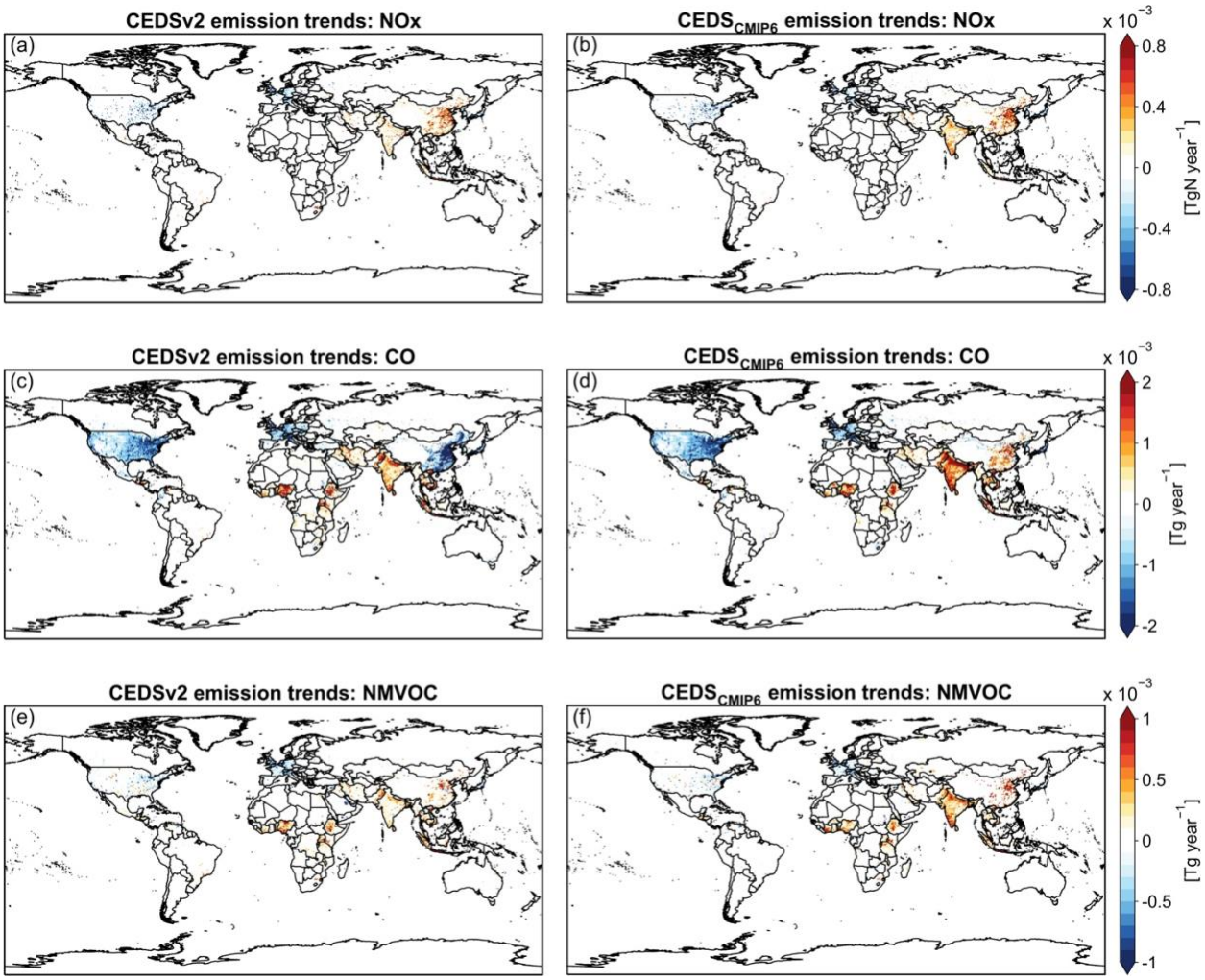

Figure S1. Comparison of spatial distributions of the total global anthropogenic NO_x, CO, and NMVOC emissions (excluding aircraft emissions) trends over 1995-2014 in the CEDSv2 inventory (left) and the $CEDS_{CMIP6}$ inventory (right). The linear trends are estimated from the ordinary linear regression method.

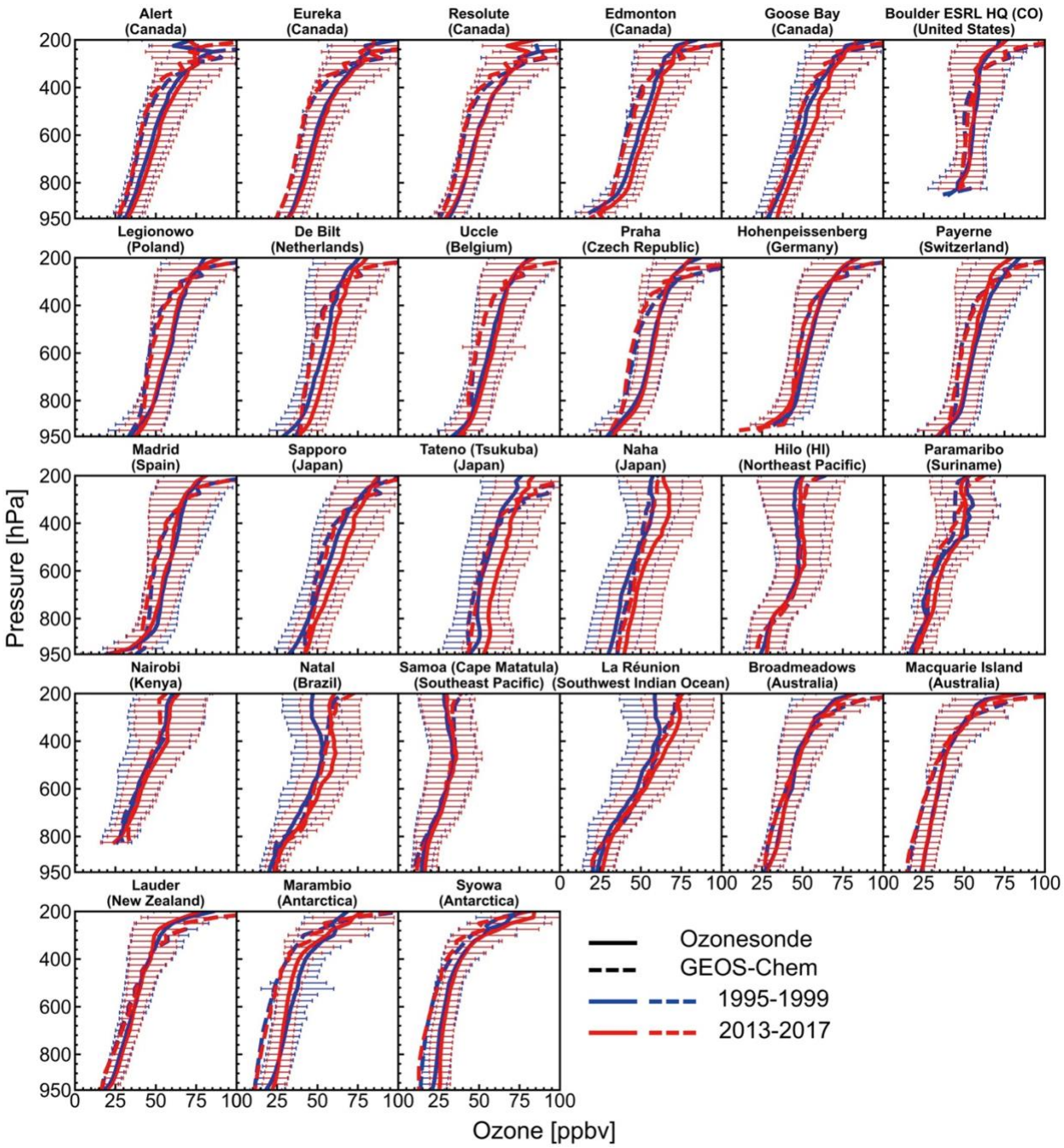

Figure S2. Same as Figure 4 but for individual sites.

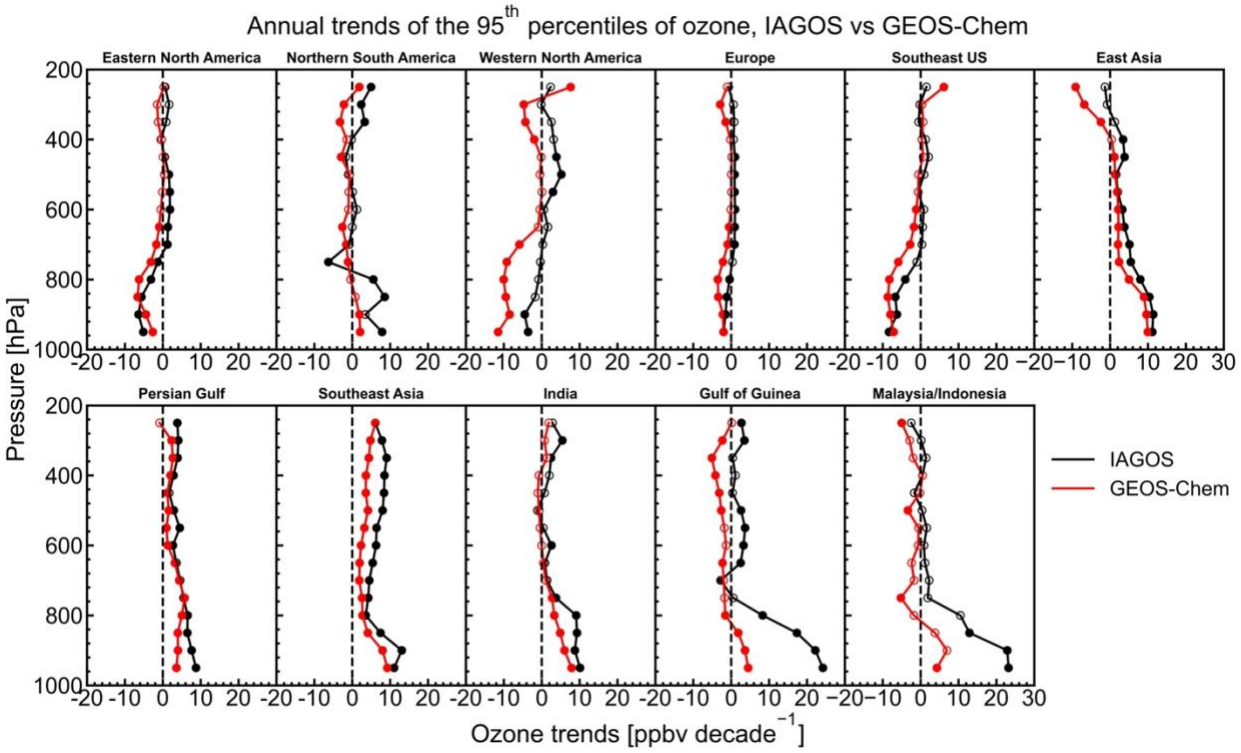

Figure S3. Same as Figure 5 but for 95th percentile ozone trends.

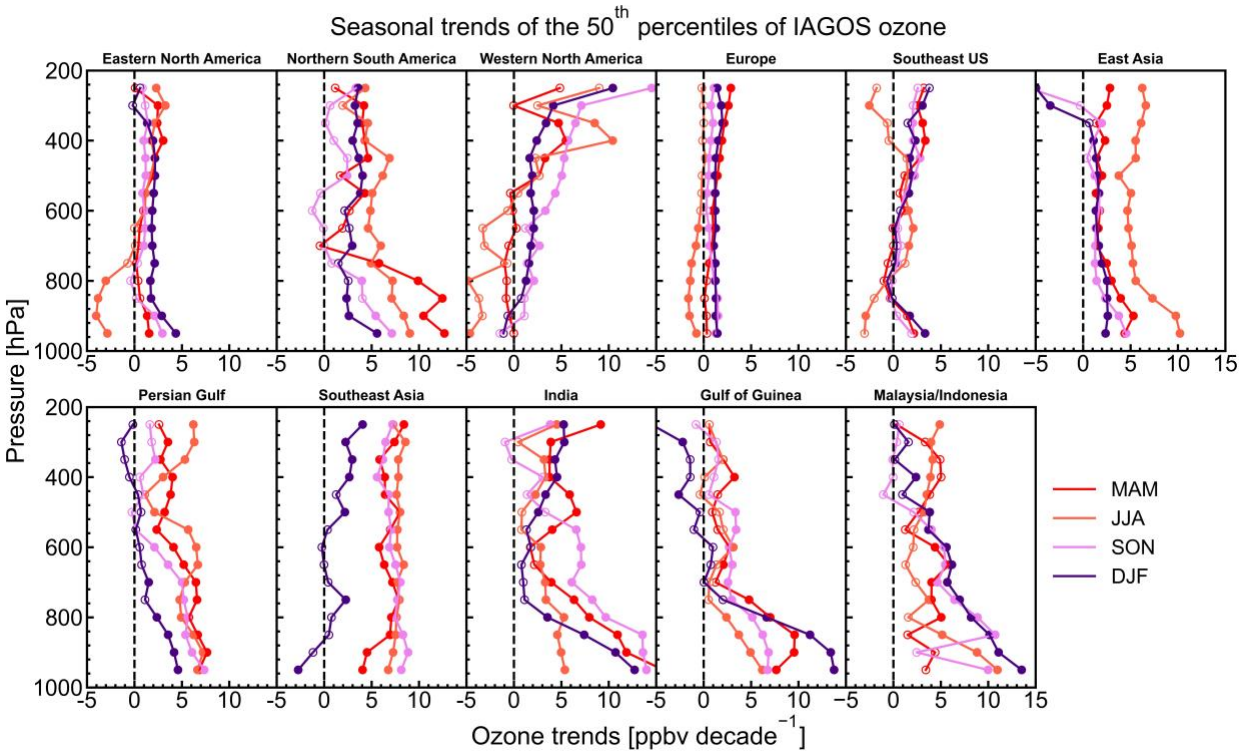

Figure S4. Same as Figure 5 but for seasonal trends of the 50th percentiles of IAGOS observed ozone.

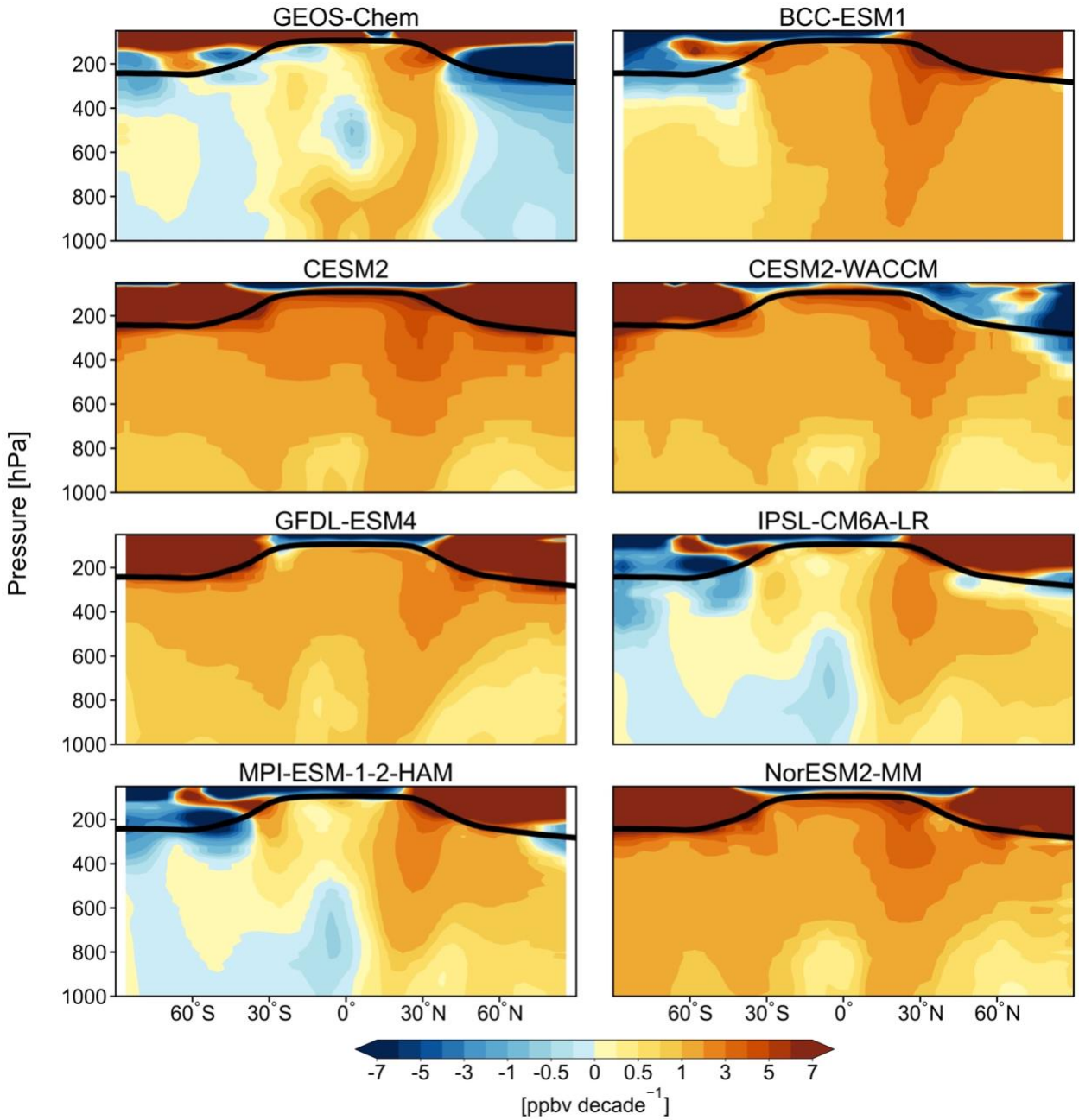

Figure S5. Comparison of the annual and zonal mean ozone trends in seven CMIP6 models with the GEOS-Chem model for the period 1995 to 2014. Black lines represent the 1995–2014 climatological annual mean tropopause from MERRA-2 reanalysis.

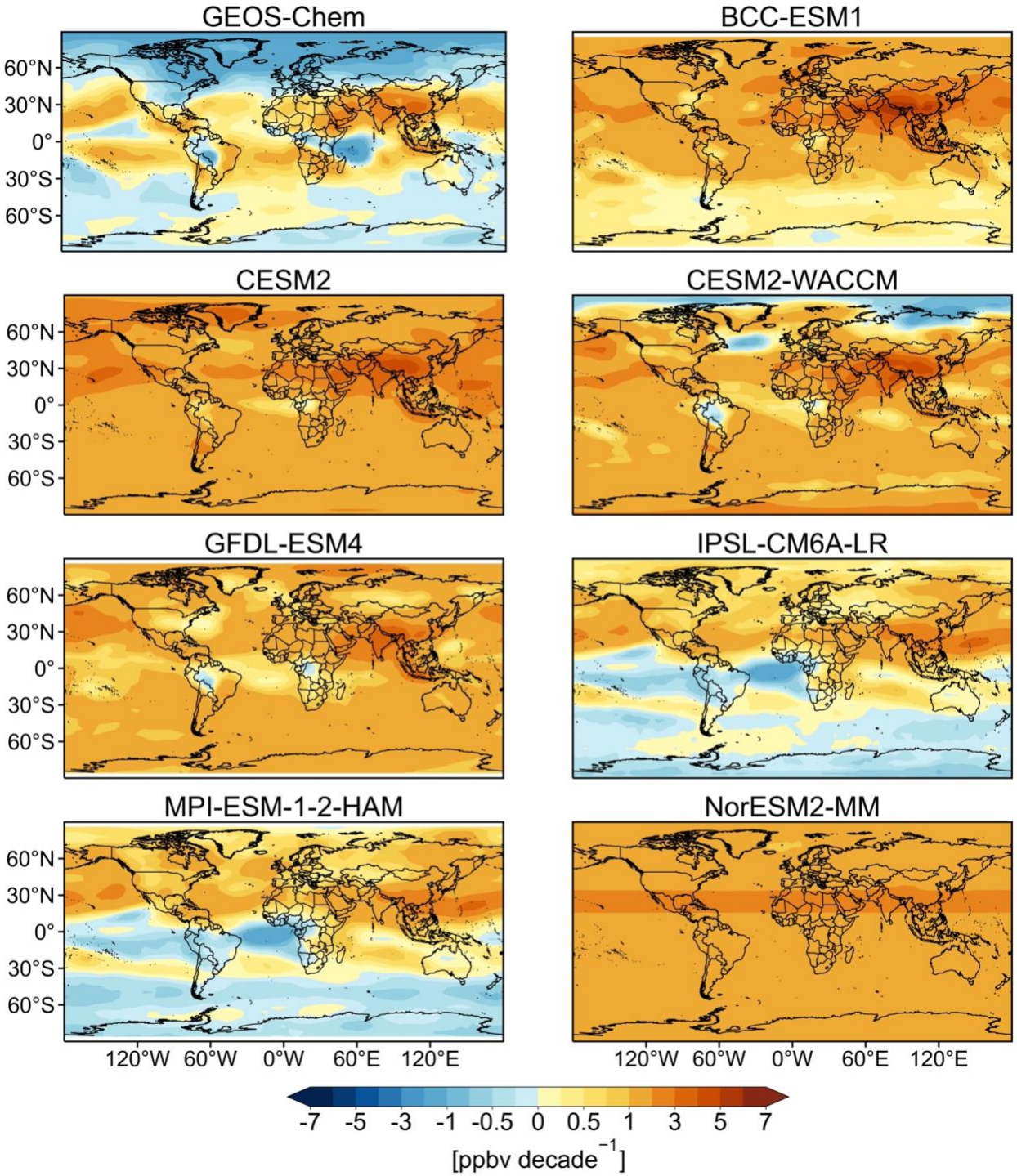

Figure S6. Comparison of the annual mean tropospheric ozone column (950-250 hPa) trends in seven CMIP6 models with the GEOS-Chem model for the period 1995 to 2014.

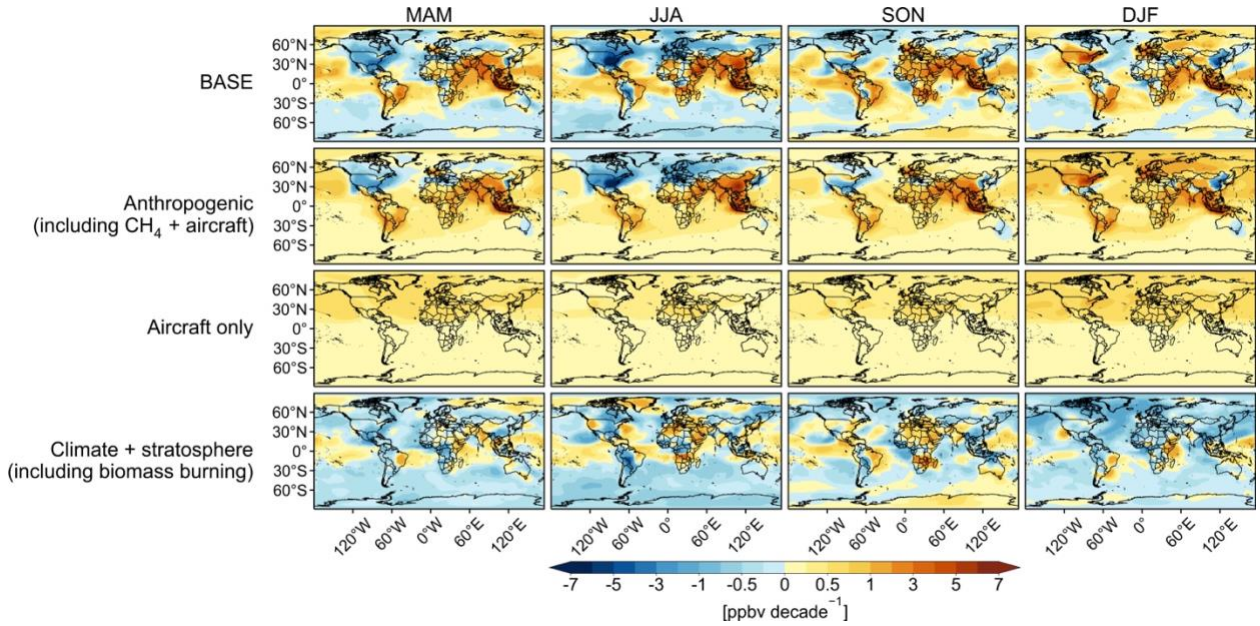

Figure S7. Same as Figure 11 but for seasonal surface ozone trends.

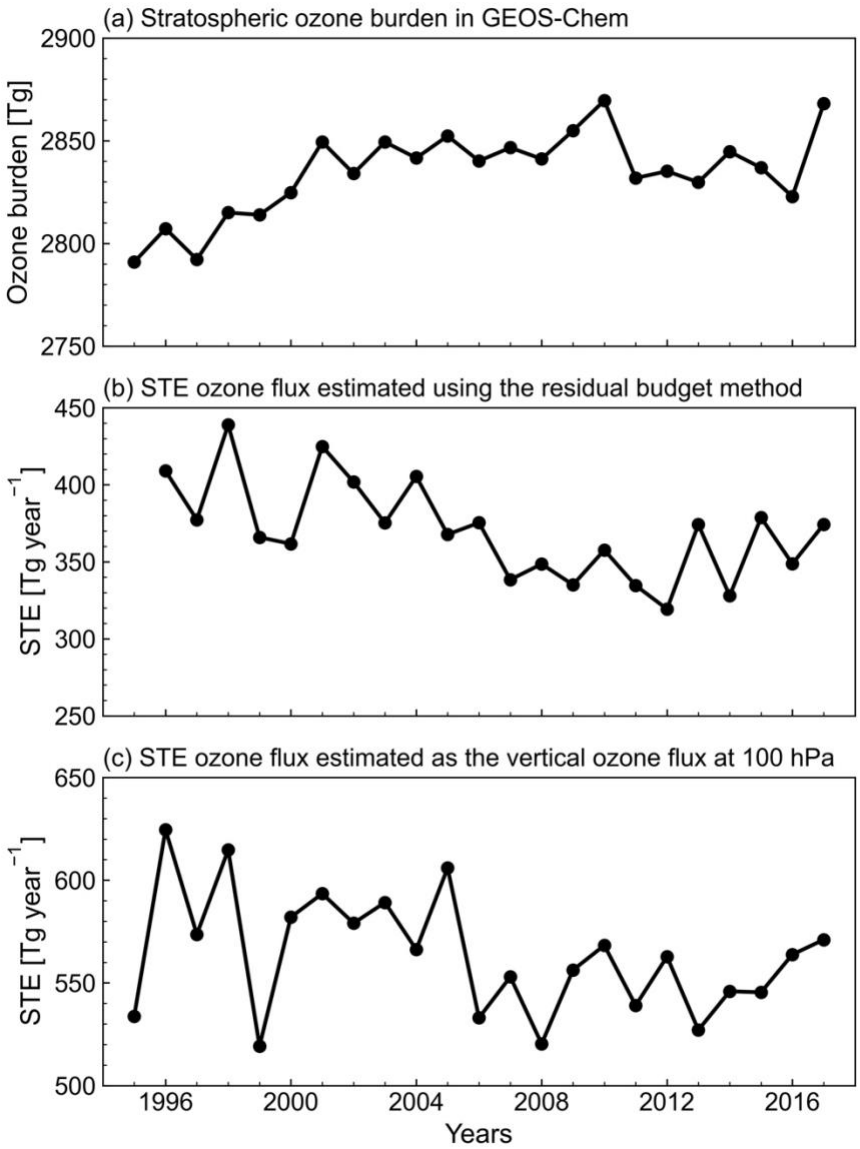

Figure S8. Evolution of GEOS-Chem stratospheric ozone burden and stratosphere-troposphere exchange (STE) ozone flux estimated by two methods in 1995-2017. Please see Section 3.3 in the text for more information.

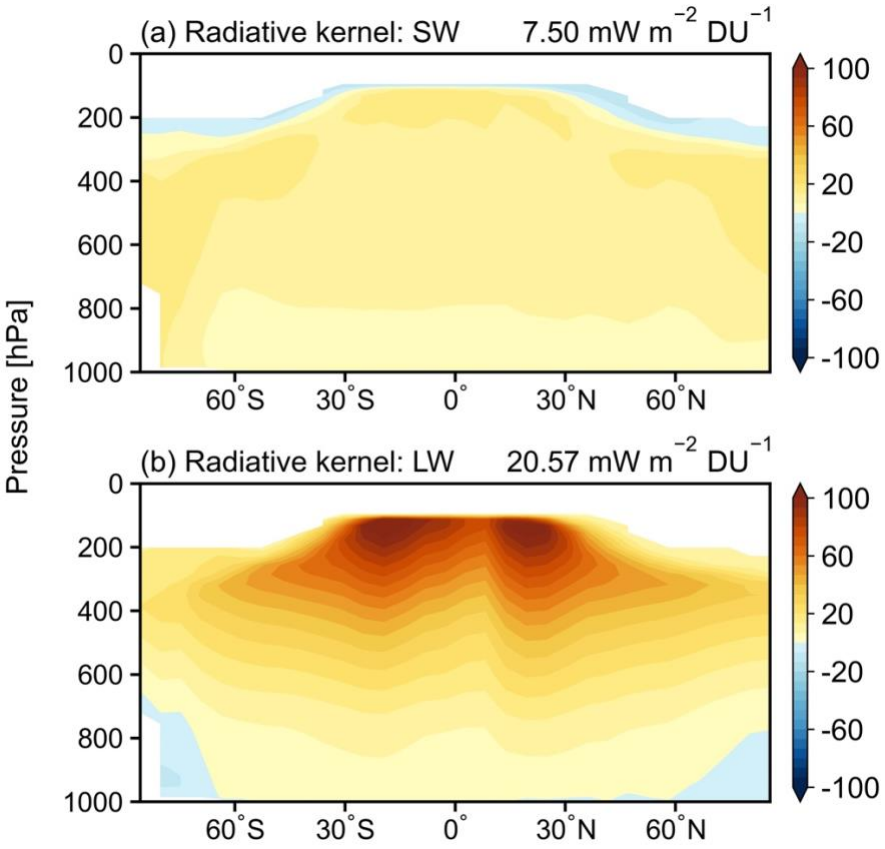

Figure S9. Annual zonal mean values of the radiative kernel (mW m^{-2} DU^{-1}) for (a) SW radiative forcing and (b) LW radiative forcing from Skeie et al. (2020). The annual global mean values are shown inset.

References

Skeie, R. B., Myhre, G., Hodnebrog, Ø., Cameron-Smith, P. J., Deushi, M., Hegglin, M. I., Horowitz, L. W., Kramer, R. J., Michou, M., Mills, M. J., Olivié, D. J. L., Connor, F. M. O., Paynter, D., Samset, B. H., Sellar, A., Shindell, D., Takemura, T., Tilmes, S., and Wu, T.: Historical total ozone radiative forcing derived from CMIP6 simulations, npj Climate and Atmospheric Science, 3, 32, 10.1038/s41612-020-00131-0, 2020.